Simple approach to fourth generation effects in $B\to X_s\ell^+\ell^-$ decay

Levent Solmaz*
Balikesir University, Physics Department (32), Balikesir, Turkey
(Received 10 October 2003; published 26 January 2004)

In a scenario in which fourth generation fermions exist, we study the effects of new physics on the differential decay width, forward-backward asymmetry, and the integrated branching ratio for $B\to X_s\ell^+\ell^-$ decay with $(\ell=e,\mu)$. The prediction of the new physics on the mentioned quantities essentially differs from the standard model results in certain regions of parameter space; the enhancement of new physics on the above-mentioned physical quantities can yield values as large as 2 times that of the SM predictions, from which present limits of experimental measurements of the branching ratio are spanned, and constraints of the new physics can be extracted. For the fourth generation CKM factor $V_{t'b}^*V_{t's}$ we use $\pm10^{-2}$ and $\pm10^{-3}$ ranges, take into consideration the possibility of a complex phase where it may bring sizable contributions, and obtain no significant dependence on the imaginary part of the new CKM factor. For the above-mentioned quantities with a new family, deviations from the SM are promising and can be used as a probe of new physics.

DOI: 10.1103/PhysRevD.69.015003 PACS number(s): 12.60.−i, 13.20.He

I. INTRODUCTION

Even if the standard model (SM) is a successful theory, one should also check probable effects that may come from potential new physics. In the SM, since we do not have a clear theoretical argument to restrict number of generations to 3, the possibility of a new generation should not be ruled out until there is certain evidence which orders us to do so. This is especially true for rare B decays, which are very sensitive to generic expansions of the SM, due to their loop structure. We know from neutrino experiments that, for the mass of the extra generations, there is a lower bound for the new generations ($m_{\nu_4}>45$ GeV) [1]. The probable effects of extra generations were studied in many works [2–16]. The existing electroweak data on the Z-boson parameters, the W boson, and the top quark masses excluded the existence of new generations with all fermions heavier than the Z-boson mass [16]; nevertheless, the same data allow a few extra generations, if one allows neutral leptons to have masses close to 50 GeV. In addition to this, recently observed neutrino oscillations require an enlarged neutrino sector [17].

Generalizations of the SM can be used to introduce a new family, which was performed previously [18]. Using similar techniques, one can search for fourth generation effects in B-meson decays. The contributions from fourth generation to rare decays have been extensively studied [19–23], where the measured decay rate has been used to put stringent constraints on the additional CKM matrix elements. In addition to $B\to X_s\gamma$, $B\to X_s\ell^+\ell^-$ can be mentioned as one of the most promising areas in search of the fourth generation, via its indirect loop effects, to constrain $V_{t'b}^*V_{t's}$ [24,25]. The restrictions of the parameter space of nonstandard models based on leading order analysis are not as sensitive as in the case of next-to-leading order analysis; hence a NLO analysis considering the possibility of a complex phase is important, which we plan to revise [26].

On the experimental side, inclusive $B\to X_s\ell^+\ell^-$ (with $\sqrt{q^2}>0.2$ GeV) decays with electron and muon modes combined $(\ell=e,\mu)$ have been observed [27,28]:

$$\mathcal{B}(B\to X_s\ell^+\ell^-)=(6.1\pm1.4^{+1.4}_{-1.1})\times10^{-6}, \tag{1}$$

$$\mathcal{B}(B\to X_s\ell^+\ell^-)=(6.3\pm1.6^{+1.8}_{-1.5})\times10^{-6}. \tag{2}$$

They are in agreement with the SM $\mathcal{B}(B\to X_s\ell^+\ell^-)_{SM}=4.2\pm0.7\times10^{-6}$ for the same cuts [29].

On the theoretical side, the situation within and beyond the SM is well settled. A collective theoretical effort has led to the practical determination of $B\to X_s\ell^+\ell^-$ at the next-to-next-to-leading order (NNLO), which was completed recently, as a joint effort of different groups (see [30–32], and references therein). It is necessary to have precise calculations also in extensions of the SM, which were performed for certain models. With the appearance of more accurate data we might be able to provide stringent constraints on free parameters of models beyond the SM. From this respect, a NNLO analysis of the new generation is important. We study the contribution of the fourth generation in the rare $B\to X_s\ell^+\ell^-$ decay at NNLO to obtain experimentally measurable quantities which are expected to appear in the forthcoming years.

The paper is organized as follows. In Sec. II, we present the necessary theoretical expressions for the $B\to X_s\ell^+\ell^-$ decay in the SM with four generations. Section III is devoted to our conclusion.

II. $B\to X_S\ell^+\ell^-$ DECAY AND FOURTH GENERATION

We use the framework of an effective low-energy theory, obtained by integrating out heavy degrees of freedoms, which were in our case the W boson and top quark and an additional t' quark. The mass of the t' is of the order of μ_W. In this approximation the effective Hamiltonian relevant for $B\to X_s\ell^+\ell^-$ decay reads [33]

*Electronic address: lsolmaz@photon.physics.metu.edu.tr; lsolmaz@balikesir.edu.tr

$$\mathcal{H}_{\rm eff}=-\frac{4G_F}{\sqrt{2}}V_{ts}^*V_{tb}\sum_{i=1}^{10}C_i(\mu)O_i(\mu), \tag{3}$$

where G_F is the Fermi coupling constant and V is the Cabibbo-Kobayashi-Maskawa (CKM) quark mixing matrix; the full set of the operators $O_i(\mu)$ and the corresponding expressions for the Wilson coefficients $C_i(\mu)$ in the SM can be found in Ref. [30].

In the model under consideration, the fourth generation is introduced in a similar way the three generations are introduced in the SM; no new operators appear and clearly the full operator set is exactly the same as in the SM, which is a rough approximation. The fourth generation changes values of the Wilson coefficients $C_i(\mu)$, $i=7,8,9,10$, via virtual exchange of the fourth generation up quark t'. With the definitions $\lambda_j=V_{js}^*V_{jb}$, where $j=u,c,t,t'$, the new physics Wilson coefficients can be written in the form

$$C_i^{4G}(\mu_W)=\frac{\lambda_{t'}}{\lambda_t}C_i(\mu_W)_{m_t\to m_{t'}}, \tag{4}$$

where the last terms in this expression describe the contributions of the t' quark to the Wilson coefficients with the replacement of m_t with $m_{t'}$. Notice that we use the definition $\lambda_{t'}=V_{t's}^*V_{t'b}$ which is an element of the 4×4 CKM matrix; from now on "4G" will stand for the sequential fourth generation model. In this model the properties of the new t' quark are the same as ordinary t, except its mass and corresponding CKM couplings. A few comments are in order here: to obtain quantitative results we need the value of the fourth generation CKM matrix element $V_{t's}^*V_{tb}$ which can be extracted, i.e., from $B\to X_s\gamma$ decay as a function of mass of the new top quark, $m_{t'}$. For this aim following [24,25], we can use the fourth generation CKM factor $\lambda_{t'}$ in the range $-10^{-2}\leqslant\lambda_{t'}\leqslant10^{-2}$. In the numerical analysis, as a first step, $\lambda_{t'}$ is assumed real and expressions are obtained as a function of the mass of the extra generation top quark $m_{t'}$. It is interesting to notice that, if we assume $\lambda_{t'}$ can have imaginary parts, experimental values can also be satisfied [23,26]. Nevertheless, if we impose the unitarity condition of the CKM matrix, we have

$$V_{us}^*V_{ub}+V_{cs}^*V_{cb}+V_{ts}^*V_{tb}+V_{t's}^*V_{t'b}=0. \tag{5}$$

With the values of the CKM matrix elements in the SM [34], the sum of the first three terms in Eq. (5) is about 7.6×10^{-2}, where the error in the sum of the first three terms is about $\pm0.6\times10^{-2}$. We assume that the value of $\lambda_{t'}$ is within this error range.

What should not be ignored in constraining $\lambda_{t'}$ is that, when adding a fourth family, the present constraints on the elements of CKM may get relaxed [34]. In order to have a clear picture of $\lambda_{t'}$, CKM matrix elements should be calculated with the possibility of a new family, using present experiments, that constitutes the CKM matrix. In this respect we do not have to exclude certain regions that violate the unitarity of the present CKM matrix, but take it in the ranges $-10^{-2}\leqslant\lambda_{t'}\leqslant10^{-2}$ and $-10^{-3}\leqslant\lambda_{t'}\leqslant10^{-3}$.

A. Differential decay width

Since extended models are very sensitive to NNLO corrections, we used the NNLO expression for the branching ratio of the radiative decay $B\to X_s\ell^+\ell^-$, which has been presented in Refs. [29,33]. In the NNLO approximation, the invariant dilepton mass distribution for the inclusive decay $B\to X_s\ell^+\ell^-$ can be written as

$$\begin{aligned}\frac{d\Gamma(b\to X_s\ell^+\ell^-)}{d\hat{s}}&=\left(\frac{\alpha_{em}}{4\pi}\right)^2\frac{G_F^2m_{b,pole}^5|V_{ts}^*V_{tb}|^2}{48\pi^3}(1-\hat{s})^2[(1+2\hat{s})\\&\times(|\tilde{C}_9^{\rm eff}|^2+|\tilde{C}_{10}^{\rm eff}|^2)+4(1+2/\hat{s})|\tilde{C}_7^{\rm eff}|^2\\&+12\,{\rm Re}(\tilde{C}_7^{\rm eff}\tilde{C}_9^{\rm eff*})],\end{aligned} \tag{6}$$

where $\hat{s}=m_{\ell^+\ell^-}^2/m_{b,pole}^2$ with ($\ell=e$ or μ). In the SM the effective Wilson coefficients $\tilde{C}_7^{\rm eff}$, $\tilde{C}_9^{\rm eff}$, and $\tilde{C}_{10}^{\rm eff}$ are given by [30,33] and can be obtained from Eqs. (8), (9), and (10), by setting $4G\to0$. Following the lines of Ali *et al.* [29] with the assumption that only the lowest nontrivial order of these Wilson coefficients gets modified by new physics, which means that $C_7^{(1)}(\mu_W)$, $C_8^{(1)}(\mu_W)$, $C_9^{(1)}(\mu_W)$, and $C_{10}^{(1)}(\mu_W)$ get modified, the shifts of the Wilson coefficients at μ_W can be written as

$$C_i(\mu_W)\to C_i(\mu_W)+\frac{\alpha_s}{4\pi}C_i^{4G}(\mu_W). \tag{7}$$

These shifts at the matching scale result in modifications of the effective Wilson coefficients,

$$\begin{aligned}\tilde{C}_7^{\rm eff}&=\left(1+\frac{\alpha_s(\mu)}{\pi}\omega_7(\hat{s})\right)\\&\times[A_7+A_{77}C_7^{4G}(\mu_W)+A_{78}C_8^{4G}(\mu_W)]\\&-\frac{\alpha_s(\mu)}{4\pi}[C_1^{(0)}F_1^{(7)}(\hat{s})+C_2^{(0)}F_2^{(7)}(\hat{s})\\&+A_8^{(0)}F_8^{(7)}(\hat{s})+A_{88}^{(0)}C_8^{4G}(\mu_W)F_8^{(7)}(\hat{s})],\end{aligned} \tag{8}$$

$$\begin{aligned}\tilde{C}_9^{\rm eff}&=\left(1+\frac{\alpha_s(\mu)}{\pi}\omega_9(\hat{s})\right)[A_9+T_9h(\hat{m}_c^2,\hat{s})\\&+U_9h(1,\hat{s})+W_9h(0,\hat{s})+C_9^{4G}(\mu_W)]\\&-\frac{\alpha_s(\mu)}{4\pi}[C_1^{(0)}F_1^{(9)}(\hat{s})+C_2^{(0)}F_2^{(9)}(\hat{s})\\&+A_8^{(0)}F_8^{(9)}(\hat{s})+A_{88}^{(0)}C_8^{4G}(\mu_W)F_8^{(9)}(\hat{s})],\end{aligned} \tag{9}$$

$$\tilde{C}_{10}^{\rm eff}=\left(1+\frac{\alpha_s(\mu)}{\pi}\omega_9(\hat{s})\right)(A_{10}+C_{10}^{4G}). \tag{10}$$

The numerical values for the parameters A_{77}, A_{78}, and $A_{88}^{(0)}$, which incorporate the effects from the running, can be found in the same reference [29]; for the functions $h(\hat{m}_c^2,\hat{s})$ and

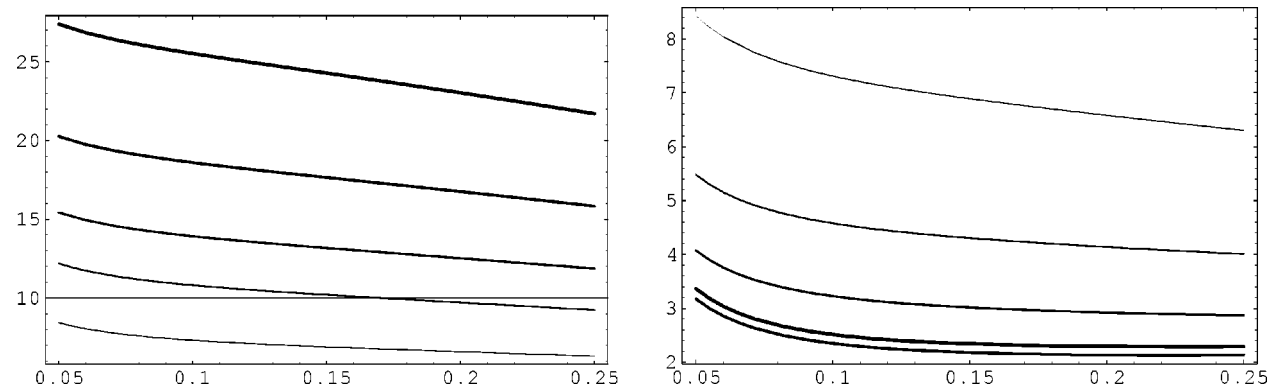

FIG. 1. Branching ratio $\mathcal{B}^{B\to X_s\ell^+\ell^-}$ $[10^{-6}]$ as a function of $\hat{s}\in[0.05,0.25]$ [see Eq. (11)]. The four thick lines show the NNLL prediction for $m_{t'}=200$, 300, 400, and 500 with increasing thickness, respectively, and the SM prediction is the thin line. The figures are obtained at the scale $\mu=5.0$ GeV. For the figure at the left, $\lambda_{t'}=-10^{-2}$, at the right, $\lambda_{t'}=10^{-2}$.

$\omega_9(\hat{s})$, they are given in Ref. [30], while $\omega_7(\hat{s})$ and $F_{1,2,8}^{(7,9)}(\hat{s})$ can be seen in Ref. [33]. In order to remove the large uncertainty coming from m_b terms it is customary to use the expression [29]

$$\mathcal{B}^{B\to X_s\ell^+\ell^-}(\hat{s})=\frac{\mathcal{B}_{\rm exp}^{B\to X_c e\bar{\nu}}}{\Gamma(B\to X_c e\bar{\nu})}\frac{d\Gamma(B\to X_s\ell^+\ell^-)}{d\hat{s}}, \tag{11}$$

which can be called the branching ratio. The explicit expression for the semileptonic decay width can be found in Ref. [30]. The branching ratio with 4G is presented in Figs. 1 and 2 for the choice of the scale $\mu=5$ GeV.

In the figures related to the dilepton invariant mass distribution we used the low region $\hat{s}\in[0.05,0.25]$ where peaks stemming from $c\bar{c}$ resonances are expected to be small. During the calculations we take $\mathcal{B}_{\rm exp}^{B\to X_c e\nu}=0.1045$.

B. Forward-backward asymmetry

We investigate both the so-called normalized and unnormalized forward-backward asymmetries with the 4G model. The double differential decay width $d^2\Gamma(b\to X_s\ell^+\ell^-)/(d\hat{s}dz)$ $[z=\cos(\theta)]$ is expressed as [31]

$$\begin{aligned}\frac{d^2\Gamma(b\to X_s\ell^+\ell^-)}{d\hat{s}\,dz}=&\left(\frac{\alpha_{em}}{4\pi}\right)^2\frac{G_F^2 m_{b,\rm pole}^5|V_{ts}^*V_{tb}|^2}{48\pi^3}(1-\hat{s})^2\left\{\frac{3}{4}[(1-z^2)+\hat{s}(1+z^2)](|\tilde{C}_9^{\rm eff}|^2+|\tilde{C}_{10}^{\rm eff}|^2)\left(1+\frac{2\alpha_s}{\pi}f_{99}(\hat{s},z)\right)\right.\\&+\frac{3}{\hat{s}}[(1+z^2)+\hat{s}(1-z^2)]|\tilde{C}_7^{\rm eff}|^2\left(1+\frac{2\alpha_s}{\pi}f_{77}(\hat{s},z)\right)-3\hat{s}z\,{\rm Re}(\tilde{C}_9^{\rm eff}\tilde{C}_{10}^{\rm eff*})\left(1+\frac{2\alpha_s}{\pi}f_{910}(\hat{s})\right)\\&\left.+6\,{\rm Re}(\tilde{C}_7^{\rm eff}\tilde{C}_9^{\rm eff*})\left(1+\frac{2\alpha_s}{\pi}f_{79}(\hat{s},z)\right)-6z\,{\rm Re}(\tilde{C}_7^{\rm eff}\tilde{C}_{10}^{\rm eff*})\left(1+\frac{2\alpha_s}{\pi}f_{710}(\hat{s})\right)\right\},\end{aligned} \tag{12}$$

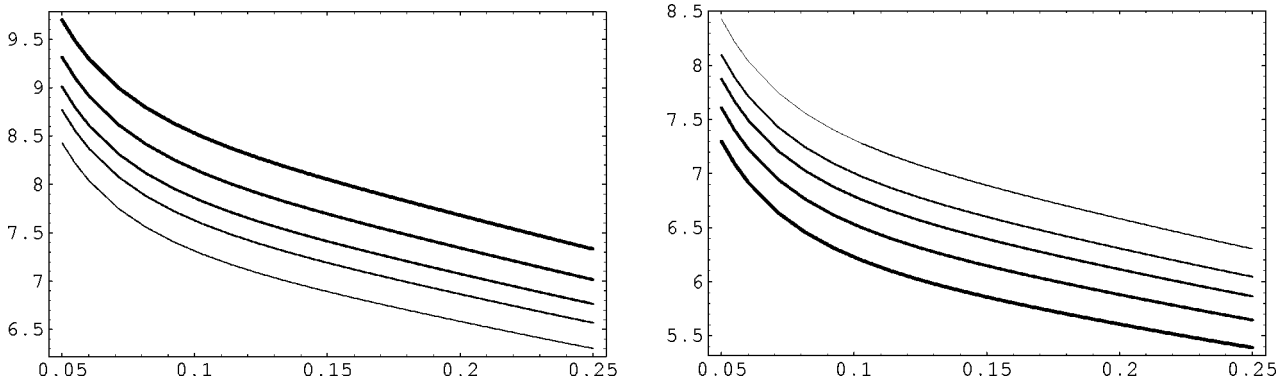

FIG. 2. The same as Fig. 1 with the choices, for the figure at the left, $\lambda_{t'}=-10^{-3}$, at the right, $\lambda_{t'}=10^{-3}$.

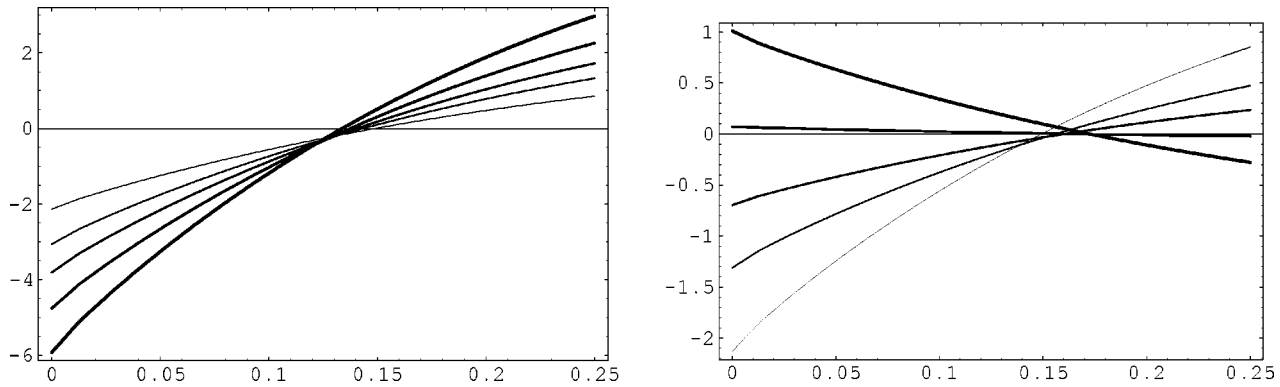

FIG. 3. Unnormalized forward-backward asymmetry $A_{\rm FB}\,[10^{-6}]$ as a function of $\hat{s}\in[0,0.25]$ [see Eq. (13)]. The four thick lines show the NNLL prediction for $m_{t'}=200$, 300, 400, and 500 with increasing thickness, respectively, and the SM prediction is the thin line. The figures are obtained at the scale $\mu=5.0$ GeV. For the figure at the left, $\lambda_{t'}=-10^{-2}$, at the right, $\lambda_{t'}=10^{-2}$.

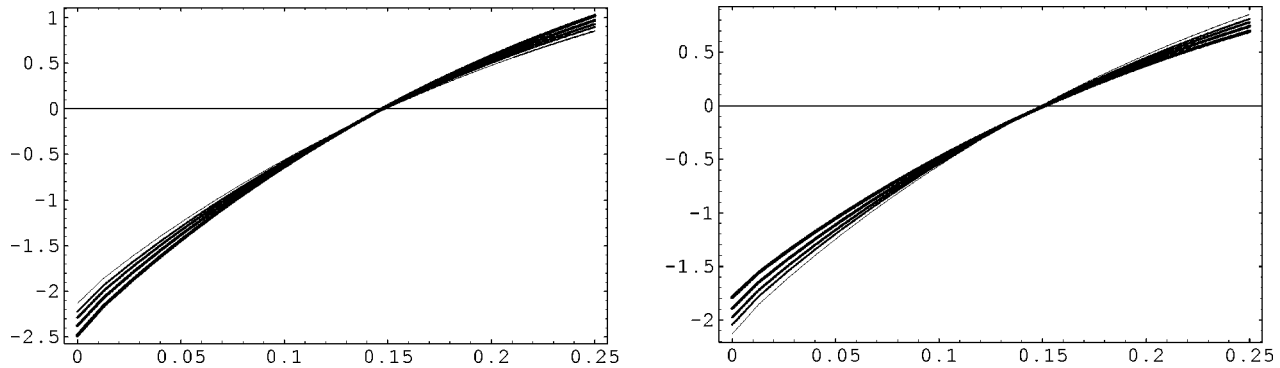

FIG. 4. Normalized forward-backward asymmetry $\overline{A_{\rm FB}}\,[10^{-6}]$ as a function of $\hat{s}\in[0,0.25]$ [see Eq. (14)]. The four thick lines show the NNLL prediction for $m_{t'}=200$, 300, 400, and 500 with increasing thickness, respectively, and the SM prediction is the thin line. The figures are obtained at the scale $\mu=5.0$ GeV. For the figure at the left, $\lambda_{t'}=-10^{-2}$, at the right, $\lambda_{t'}=10^{-2}$.

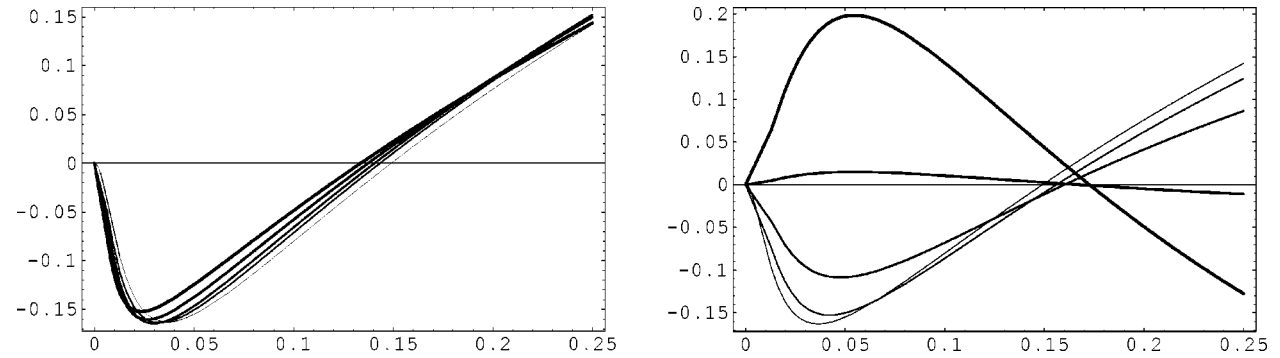

FIG. 5. The same as Fig. 3 with the choices for the figure at the left, $\lambda_{t'}=-10^{-3}$, at the right, $\lambda_{t'}=10^{-3}$.

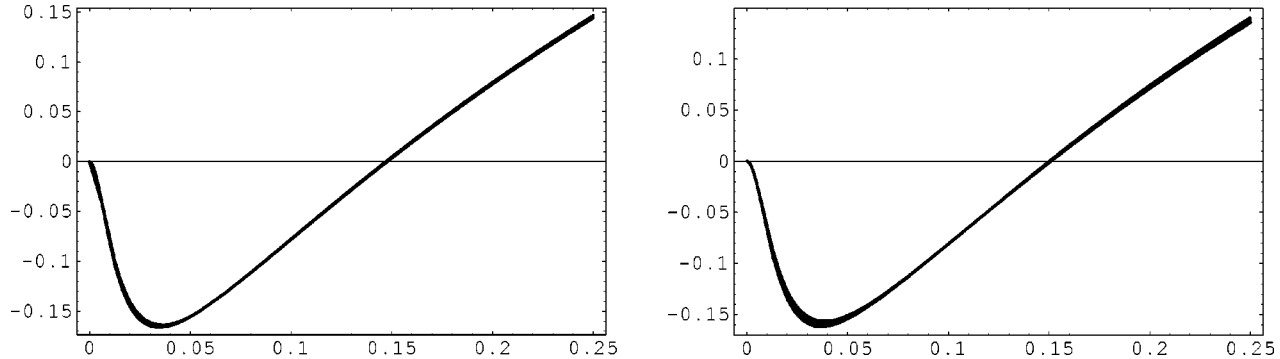

FIG. 6. The same as Fig. 4 with the choices, for the figure at the left, $\lambda_{t'}=-10^{-3}$, at the right, $\lambda_{t'}=10^{-3}$.

TABLE I. Numerical values of the coefficients a_i (evaluated at $\mu_b=5$ GeV) for the decays $B\to X_s\ell^+\ell^-$ ($\ell=e,\mu$), taken from Ref. [29].

ℓ	a_1	a_2	a_3	a_4	a_5	a_6	a_7	a_8	a_9	a_{10}
e	1.9927	6.9357	0.0640	0.5285	0.6574	0.2673	−0.0586	0.4884	0.0095	−0.5288
μ	2.3779	6.9295	0.0753	0.6005	0.7461	0.5955	−0.0600	0.5828	0.0102	−0.6225

where θ is the angle between the momenta of the b quark and the ℓ^+, measured in the rest frame of the lepton pair. The functions $f_{99}(\hat{s},z)$, $f_{77}(\hat{s},z)$, $f_{910}(\hat{s})$, $f_{79}(\hat{s},z)$, and $f_{710}(\hat{s})$ are the analogues of $\omega_{99}(\hat{s})$, $\omega_{77}(\hat{s})$, and $\omega_{79}(\hat{s})$ which can be found in the same reference [31].

The unnormalized version of the forward-backward asymmetry, $A_{\rm FB}(\hat{s})$, is defined as

$$A_{\rm FB}(\hat{s})=\frac{\displaystyle\int_{-1}^{1}\frac{d^2\Gamma(b\to X_s\ell^+\ell^-)}{d\hat{s}\,dz}\,{\rm sgn}(z)dz}{\Gamma(B\to X_c e\bar{\nu}_e)}\mathcal{B}_{\rm exp}^{B\to X_c e\bar{\nu}}, \tag{13}$$

while the definition of the normalized forward-backward asymmetry $\bar{A}_{\rm FB}(\hat{s})$ reads

$$\bar{A}_{\rm FB}(\hat{s})=\frac{\displaystyle\int_{-1}^{1}\frac{d^2\Gamma(b\to X_s\ell^+\ell^-)}{d\hat{s}\,dz}\,{\rm sgn}(z)dz}{\displaystyle\int_{-1}^{1}\frac{d^2\Gamma(b\to X_s\ell^+\ell^-)}{d\hat{s}\,dz}dz}. \tag{14}$$

The position of the zero of the $A_{FB}(\hat{s}_0)=0$ is very sensitive to 4G effects as it is seen in Figs. 3 and 4. However, as the 4G parameter $\lambda_{t'}$ decreases, expectations of the new model are getting closer to SM values which can be inferred from Figs. 5 and 6.

C. Integrated branching ratio

By a suitable choice of integration limits over $\hat{s}$ one can obtain an integrated branching ratio in accordance with the experiment for e and μ, which has been already performed; hence we use the integrated branching ratio expression which has the form [29]

$$\begin{aligned}\mathcal{B}(B\to X_s\ell^+\ell^-)&=10^{-6}\times[a_1+a_2|A_7^{\rm tot}|^2+a_3(|C_9^{\rm 4G}|^2+|C_{10}^{\rm 4G}|^2)\\&+a_4\,{\rm Re}\,A_7^{\rm tot}{\rm Re}\,C_9^{44G}+a_5\,{\rm Im}\,A_7^{\rm tot}\,{\rm Im}\,C_9^{\rm 4G}+a_6\,{\rm Re}\,A_7^{\rm tot}\\&+a_7\,{\rm Im}\,A_7^{\rm tot}+a_8\,{\rm Re}\,C_9^{\rm 4G}+a_9{\rm Im}\,C_9^{\rm 4G}+a_{10}\,{\rm Re}\,C_{10}^{\rm 4G}],\end{aligned} \tag{15}$$

where the numerical values of the coefficients a_i are given in Table I for $\ell=e,\mu$. For the integrated branching ratios we refer to Figs. 7 and 8 of electron and muon, respectively.

III. DISCUSSION

In the sequential fourth generation model, there are basically two free parameters: the mass of new generations and CKM factors which can have imaginary phases. As a worst scenario, we decompose $\lambda_{t'}={\rm Re}[\lambda_{t'}]+I\times{\rm Im}[\lambda_{t'}]$ and choose the range ${\rm Im}[\lambda_{t'}]/{\rm Re}[\lambda_{t'}]\leqslant 10^{-2}$; we checked the effect of this choice and observe that the contribution from the imaginary part can be neglected for all kinematical observables. Naturally, these quantities should be fixed by respecting experiments. Besides, constraints for CKM values should be updated by noting that the existence of a new generation can relax the matrix elements of ${\rm CKM}_{3\times3}$ when it is accepted as a submatrix of ${\rm CKM}_{4\times4}$.

Since the scale dependence of NNLO calculations of $B\to X_s\ell^+\ell^-$ are not very high [31], during the calculations we set the scale $\mu=5$ GeV and use the main input parameters as follows:

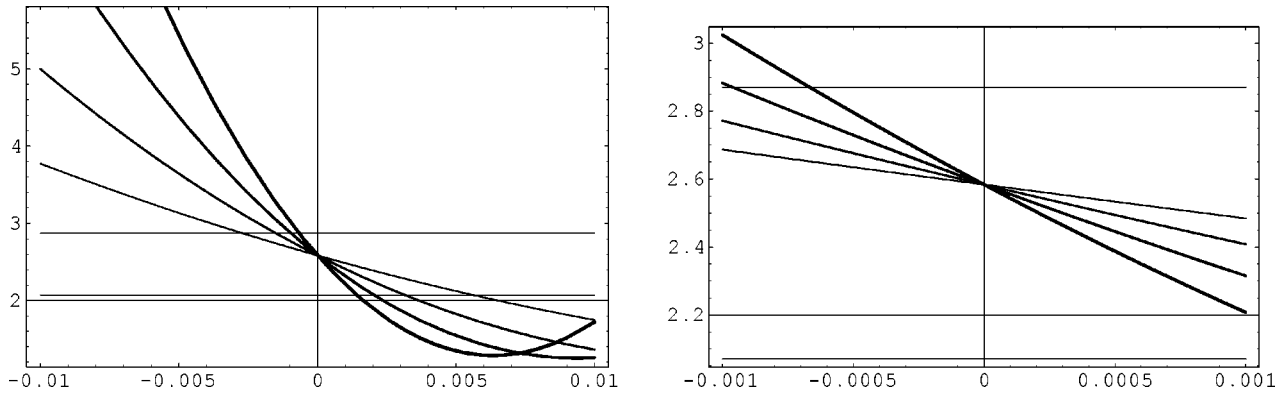

FIG. 7. Integrated branching ratio $\mathcal{B}(B\to X_s\ell^+\ell^-)$ $[10^{-6}]$ as a function of $\lambda_{t'}$ for $\ell=e$ [see Eq. (15)]. In the left figure $\lambda_{t'}\in[-10^{-2},10^{-2}]$. For the figure at the right $\lambda_{t'}\in[-10^{-3},10^{-3}]$. In the figures straight lines show the SM allowed region.

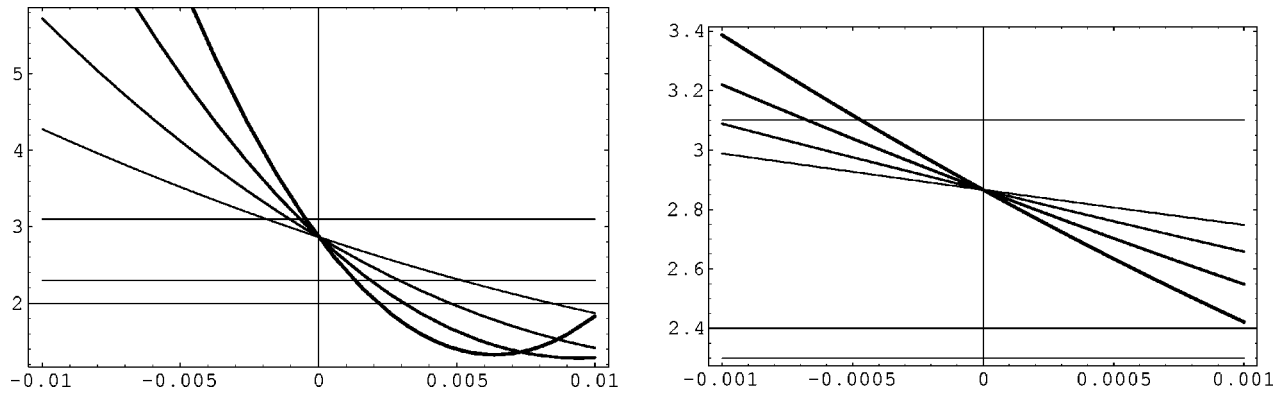

FIG. 8. Integrated branching ratio $\mathcal{B}(B\to X_s\ell^+\ell^-)\,[10^{-6}]$ as a function of $\lambda_{t'}$ for $\ell=\mu$. In the left figure $\lambda_{t'}\in[-10^{-2},10^{-2}]$. For the figure at the right $\lambda_{t'}\in[-10^{-3},10^{-3}]$. In the figures straight lines show the SM region.

$$\alpha_{em}=1/133,\alpha_s(m_Z)=0.119,$$

$$G_F=1.16639\times10^{-5}\ \text{GeV}^{-2},\quad m_W=80.33\ \text{GeV},$$

$$m_b=4.8\ \text{GeV},\quad m_t=176\ \text{GeV},\quad m_c=1.4\ \text{GeV},$$

and Wolfenstein parameters:

$$A=0.75,\quad \lambda=0.221,\quad \rho=0.4,\quad \eta=0.2. \tag{16}$$

The effects of new physics on kinematical observables can be summarized as follows.

(i) The differential decay width $\mathcal{B}^{B\to X_s\ell^+\ell^-}$ is presented in Figs. 1 and 2, where it is shown that SM predictions can be strongly enhanced with a new quark for the choice $\lambda_{t'}<0$. It is also possible to suppress the decay width for positive solutions of $\lambda_{t'}$ which is not favored.

(ii) Forward-backward asymmetry is also very sensitive to 4G effects, especially for the choice $\lambda_{t'}=10^{-2}$. As is seen in Figs. 3 and 4, as the mass of $m_{t'}$ increases, it is even possible to have positive values for $A_{FB}(0)$ which is in contradiction with the SM, but natural in extended models. Once the experimental results related to this quantity are obtained, it will be a keen test of the fourth generation model. Deviations from the point $\hat{s}=0$ are detectable as is seen in Fig. 5 for the choice of $\lambda_{t'}\in[-10^{-3},10^{-3}]$, whereas for the same region we see almost no dependence on the normalized forward-backward asymmetry in Fig. 6. While the standard model states the central value $A_{\rm FB}^{\rm NNLO}(0)=-(2.30\pm0.10)\times10^{-6}$, 4G predictions cover the range $A_{\rm FB}^{\rm 4G,NNLO}(0)\in[-6,1]\times10^{-6}$ for the choices $\lambda_{t'}=-10^{-2},10^{-2}$, respectively. For the point where forward-backward asymmetry vanishes the standard model result is $\hat{s}_0^{\rm NNLO}=0.162\pm0.002$; however, 4G predictions are roughly $\hat{s}_0^{\rm 4G,NNLO}\in[0.13,0.18]$.

(iii) The integrated branching ratios, Figs. 7 and 8, strongly depend on the new physics parameters $\lambda_{t'}$ and $m_{t'}$; therefore, it is possible to restrict them by respecting experiments. As can be deduced from the figures, when 4G effects are switched off our calculations are lying on the SM ground within error bars [29]. Similar to the branching ratio for integrated branching ratios enhancement comes from negative choices of $\lambda_{t'}$ which favors smaller values for $A_{\rm FB}^{\rm SM,NNLO}(0)=-(2.30\pm0.10)\times10^{-6}$.

To summarize, in this work we present the predictions of the sequential fourth generation model for experimentally measurable quantities related to $B\to X_s\ell^+\ell^-$ decay which is expected to emerge in the near future thanks to running B factories. These predictions differ from the SM in certain regions and hence can be used to differentiate the existence of the fourth family or to put stringent constraints on the free parameters of the model, if it exists.

[1] DELPHI Collaboration, P. Abreu *et al.*, Phys. Lett. B **274**, 23 (1992).
[2] X.G. He and S. Paksava, Nucl. Phys. **B278**, 905 (1986).
[3] A. Anselm *et al.*, Phys. Lett. **156B**, 103 (1985).
[4] U. Turke *et al.*, Nucl. Phys. **B258**, 103 (1985).
[5] I. Bigi, Z. Phys. C **27**, 303 (1985).
[6] G. Eilam, J.L. Hewett, and T.G. Rizzo, Phys. Rev. D **34**, 2773 (1986).
[7] W.S. Hou and R.G. Stuart, Phys. Rev. D **43**, 3669 (1991).
[8] N.G. Deshpande and J. Trampetic, Phys. Rev. D **40**, 3773 (1989).
[9] G. Eilam, B. Haeri, and A. Soni, Phys. Rev. D **41**, 875 (1990); Phys. Rev. Lett. **62**, 719 (1989).
[10] N. Evans, Phys. Lett. B **340**, 81 (1994).
[11] P. Bamert and C.P. Burgess, Z. Phys. C **66**, 495 (1995).
[12] T. Inami *et al.*, Mod. Phys. Lett. A **10**, 1471 (1995).
[13] A. Masiero *et al.*, Phys. Lett. B **355**, 329 (1995).
[14] V. Novikov *et al.*, Mod. Phys. Lett. A **10**, 1915 (1995); **11**, 687(E) (1996); Rep. Prog. Phys. **62**, 1275 (1999).
[15] J. Erler and P. Langacker, Eur. Phys. J. C **3**, 90 (1998).
[16] M. Maltoni *et al.*, Phys. Lett. B **476**, 107 (2000).
[17] P.H. Frampton, P.Q. Hung, and M. Sher, Phys. Rep. **330**, 263 (2000); J.I. Silva-Marcos, J. High Energy Phys. **12**, 036 (2002).
[18] J.F. Gunion, D. McKay, and H. Pois, Phys. Rev. D **51**, 201 (1995).

[19] W.S. Hou, A. Soni, and H. Steger, Phys. Lett. B **192**, 441 (1987).
[20] W.S. Hou, R.S. Willey, and A. Soni, Phys. Rev. Lett. **58**, 1608 (1987); **60**, 2337(E) (1987).
[21] T. Hattori, T. Hasuike, and S. Wakaizumi, Phys. Rev. D **60**, 113008 (1999); T.M. Aliev, D.A. Demir, and N.K. Pak, Phys. Lett. B **389**, 83 (1996); Y. Dincer, *ibid.* **505**, 89 (2001) and references therein.
[22] C.S. Huang, W.J. Huo, and Y.L. Wu, Mod. Phys. Lett. A **14**, 2453 (1999); Phys. Rev. D **64**, 016009 (2001).
[23] T.M. Aliev, A. Özpineci, and M. Savci, Eur. Phys. J. C **29**, 265 (2003).
[24] Huang, Huo, and Wu, the first citation of Ref. [22].
[25] T.M. Aliev *et al.*, Nucl. Phys. **B585**, 275 (2000).
[26] L. Solmaz, hep-ph/0204016.
[27] Belle Collaboration, J. Kaneko *et al.*, Phys. Rev. Lett. **90**, 021801 (2003).
[28] BABAR Collaboration, B. Aubert, hep-ex/0308016.
[29] A. Ali *et al.*, Phys. Rev. D **66**, 034002 (2002).
[30] C. Bobeth, M. Misiak, and J. Urban, Nucl. Phys. **B574**, 291 (2000).
[31] H.M. Asatrian *et al.*, Phys. Rev. D **66**, 094013 (2002).
[32] A. Ghinculov *et al.*, Nucl. Phys. **B648**, 254 (2003).
[33] H.H. Asatrian, H.M. Asatrian, C. Greub, and M. Walker, Phys. Lett. B **507**, 162 (2001); Phys. Rev. D **65**, 074004 (2002).
[34] Particle Data Group, C. Caso *et al.*, Eur. Phys. J. C **3**, 1 (1998).